

Effect of Temperature on the Formation of Microporous PVDF Membranes by Precipitation from 1-Octanol/DMF/PVDF and Water/DMF/PVDF Systems

Liao-Ping Cheng*

Department of Chemical Engineering, Tamkang University, Taipei, Taiwan, R.O.C. 25137

Received March 22, 1999; Revised Manuscript Received July 13, 1999

ABSTRACT: The effects of precipitation temperature on the morphology and crystal structure of PVDF membranes formed in a wet phase inversion process were studied. The liquid–liquid demixing line (binodal) and gelation phase boundaries of the systems were determined over the temperature range 25–85 °C. As the temperature was raised, the crystallization-induced gelation line was found to approach and/or intersect the binodal, leading to a favored situation for liquid–liquid demixing to dominate the initial stage of precipitation. This was well demonstrated in the cellular asymmetric morphology as observed by SEM and AFM imaging. The top surface of this membrane was composed of stacks of crystalline lamellae, with interlamellar distance estimated to be 13–20 nm by AFM. At lower temperatures (e.g., 25 °C), the membrane solution precipitated into a uniform morphology composed of spherical crystallites that exhibited the “ β ” form (type I) crystal structure, as was evidenced by the WAXD analysis. By contrast, when PVDF was precipitated at higher temperatures (e.g., 65 °C) from 1-octanol/DMF, the formed membrane became largely in the “ α ” form (type II) crystal structure.

Introduction

For membranes synthesized from semicrystalline polymers, the sequence and the extent of the phase separation events, e.g., liquid–liquid demixing, crystallization, gelation, etc., in the precipitation process are known to dictate the ultimate porous structures in the formed membranes. In general, when liquid–liquid demixing precedes crystallization, various cellular structures result, whose pores, either sponge- or fingerlike, are formed from growth of the polymer-poor phase within the matrix of the polymer-rich phase.^{1–6} In certain preparation conditions, crystallization can be enhanced to dominate the precipitation process, thereby yielding particulate morphologies composed of crystalline particles, which interlinked into a uniform mat.^{1–6} Ordinarily, however, crystallization is much slower than liquid–liquid demixing, owing to the process of reorientation of polymer molecules into the crystalline lattice, and thus, membranes with particulate morphology can be produced only in a restricted window wherein liquid–liquid demixing is sufficiently suppressed.

There are many formation parameters that affect polymer precipitation and ultimately the morphology of the precipitated membranes. Of all these parameters, the composition of the casting solution, the harshness of the precipitation bath, and the precipitation temperature are most influential and are, therefore, most frequently discussed in the literature.^{1–15} In the present study, we have focused our attention on the effect of temperature, with other factors being fixed. Using the isothermal immersion–precipitation method, membranes could be tailored into either more cellular or particulate morphologies simply by varying the system temperature. This suggests that the role of dominance by either liquid–liquid demixing or crystallization can be reverted depending on the precipitation temperature.

Quite interestingly, it was found that such a temperature effect could be correlated with the phase behavior of current systems. This was made possible by selecting casting dopes that were in the “incipient precipitation” state with respect to crystallization and coagulation baths that were very weak nonsolvents at low temperatures. In this condition, crystallization was found to occur almost exclusively in the absence of liquid–liquid demixing. On the other hand, these specific dope and bath conditions became favorable to the liquid–liquid demixing process at elevated temperatures, owing to the system's phase behavior.

The phase diagrams of water/DMF/PVDF and 1-octanol/DMF/PVDF at 25 °C have been reported previously.^{5,14} For either system, the liquid–liquid demixing line (i.e., binodal) is located inside the crystallization-induced gelation line, and there exists a wide region where crystallization can occur in the absence of liquid–liquid demixing. At elevated temperatures, however, the situation alters; as shown in Figure 1, the gelation line approaches and even intersects the binodal. This results in a much smaller crystallization zone, yet the liquid–liquid demixing region contracted only slightly. In other words, liquid–liquid demixing could occur prior to crystallization at high temperatures, which was confirmed by the morphologies of the membranes, as examined by SEM and AFM imaging. In addition, the crystalline characters of the membranes, being identified using the wide-angle X-ray diffraction method, indicated that different precipitation temperatures yielded membranes with different crystal structures.

Materials and Methods

Materials. PVDF (Kynar 740, Elf Atochem: intrinsic viscosity = 0.881 dL/g, M_n = 254 000 g/mol) was obtained in pellet form. The terpolymer of vinylidene fluoride, hexafluoropropylene, and tetrafluoroethylene (Kynar 9301, VDF/HFP/TFE = 60/20/20, intrinsic viscosity = 0.4 dL/g, M_n = 79 200 g/mol) was supplied free of charge by Elf Atochem Inc. DMF (Baker Analyzed, reagent grade, 98 wt %, d = 0.944 g/mL)

* Corresponding author.

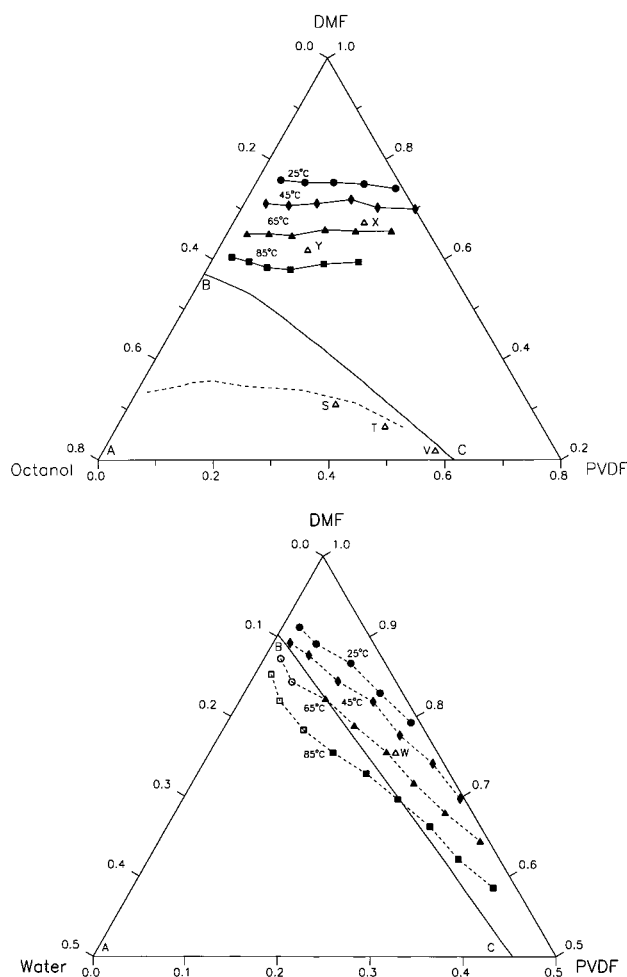


Figure 1. Phase diagrams of (a, top) 1-octanol/DMF/PVDF and (b, bottom) water/DMF/PVDF systems at various temperatures: ●, measured gelation data at 25 °C; ◆, measured gelation data at 45 °C; ▲, measured gelation data at 65 °C; ■, measured gelation data at 85 °C; ○, measured binodal at 65 °C; □, measured binodal at 85 °C. Region "ABC": computed binodal; - - -: measured binodal for 1-octanol/DMF/PVDF terpolymer. Compositions are in weight fractions.

was used as the solvent. Both double distilled–deionized water and 1-octanol (Reidel-de Haen, reagent grade, $d = 0.82$ g/mL) were used as the nonsolvents. All materials were used as received.

Gelation and Liquid–Liquid Demixing Boundaries. The gelation and liquid–liquid demixing boundaries were determined by the cloud point method.^{5,13,14} A specific amount of crystalline PVDF (Kynar 740, dried in a vacuum oven at 70 °C) was mixed with a suitable amount of DMF in a sealed Teflon-lined bottle. The mixture was then blended at room temperature until polymer was sufficiently swelled. To this solution was added a known quantity of nonsolvent. This mixture was agitated in a roll mill (at 110 °C) until a clear homogeneous solution was obtained. To examine the effect of temperature on the phase behavior, the solutions were placed in an isothermal thermostat which was maintained at 25, 45, 65, and 85 °C for a period of 2 weeks. For samples with different nonsolvent contents at different temperatures, three types of phase-separated results were observed: (i) the solution precipitated into a translucent gel; (ii) the solution underwent liquid–liquid-phase separation into two clear liquid phases; (iii) with prolonged times, some solutions changed to a clear liquid coexisting with a gel, i.e., both liquid–liquid demixing and gelation have occurred. The equilibrium gelation point (case i) and the binodal (case ii) were identified as the compositions at which homogeneous solutions began to separate into equilibrium phases.

DSC Characterization of Gels. The thermal properties of the crystalline PVDF gels (case i) were studied using a differential scanning calorimeter (Netsche, DSC 200) over the temperature range 35–90 °C at various heating rates.

Membrane Preparation and Characterization. Membranes were prepared using the direct immersion–precipitation method. A homogeneous dope composed of PVDF, DMF, and water was spread uniformly on a glass plate and then coagulated in a bath containing pure nonsolvent or a mixture of nonsolvent and solvent to form a laminate. Compositions of the dopes are shown in the phase diagram in Figure 1. Dope "X" (PVDF: 23 wt %, DMF: 67 wt %, water: 10 wt %) and "W" (PVDF: 20 wt %, DMF: 75.5 wt %, water: 4.5 wt %) were solutions in the state of "incipient precipitation" with respect to PVDF crystallization. These dopes were commonly observed to precipitate over a period of storage. They had to be heated to complete dissolution and then cooled to the desired temperature before immersing into the bath. To investigate the effect of temperature on the membrane structure, precipitation was carried out at three different temperatures: 25, 45, and 65 °C. Both the glass plate and the precipitation medium were kept at the same temperature as the polymer solution. The residual nonsolvent and solvent in the nascent membrane were extracted by a series of soaking steps. The membranes were then dried in a press at ca. 65 °C. Characterization of the membranes was carried out using the following methods: (1) The surfaces and interior structures of the dried membranes were examined using SEM (S800, Hitachi). (2) The crystalline character of the membranes was determined using the wide-angle X-ray diffraction method. (3) The lamellar structure and the interlamellar distance were observed using an atomic force microscope (SPM, Digital Instrument).

Trajectory and Concentration Profile Calculation. The local concentration of each component in the membrane solution and the precipitation bath was computed using a scheme developed previously.^{4,14} The input parameters for calculations can be found in Table 1 of ref 13. The calculated concentration profiles were plotted on the phase diagram to obtain the diffusion trajectories.

Results

Phase Diagrams of 1-Octanol–DMF–PVDF and Water–DMF–PVDF. Phase diagrams of 1-octanol/DMF/PVDF and water/DMF/PVDF systems over the range 25–85 °C are given in Figure 1, a and b, respectively. The filled circles represent the measured compositions at which gelation first observed at 25 °C. These data points form a gelation boundary, below which crystallization-induced gelation will ultimately occur for an initially uniform solution. The crystalline character of the gels has been described previously using the DSC and SALS (small-angle light scattering) methods.^{5,14} As the temperature was raised, gels that were formed at lower temperatures may gain enough thermal energy to fuse into homogeneous solutions. Hence, the gelation boundaries shift downward with increasing temperature and the one-phase region becomes larger, as shown in Figure 1. DSC measurements of several gels were performed to confirm the gelation boundaries observed visually. The melting endotherms of two such samples, corresponding to open triangle points "X" and "Y" in Figure 1a, are shown in Figure 2. The initial melting temperatures of the endotherms appear to be consistent with the observed gelation temperatures in Figure 1a. It is interesting to notice that the isotherms at different temperatures are roughly parallel to each other. This phenomenon was also observed in the system of water/DMSO/EVAL copolymer.¹³ The pure liquid–liquid demixing phenomenon in the absence of crystallization (i.e., case ii described in the experimental section) was not observed in the 1-octanol/DMF/PVDF

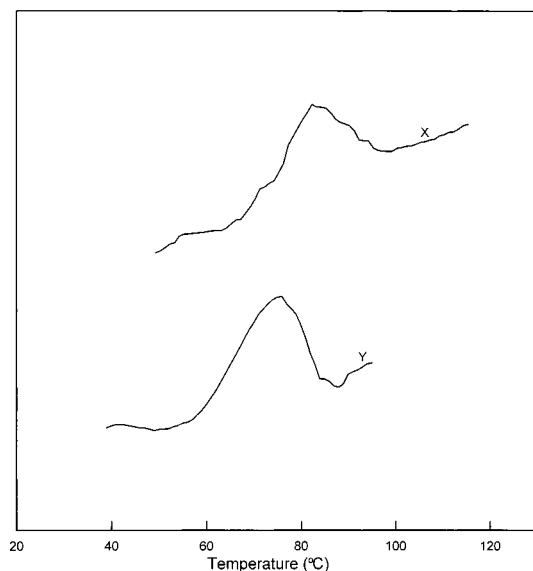


Figure 2. DSC thermograms of crystalline gels: X, point "X" in Figure 1a; Y, point "Y" in Figure 1a. Scanning rate was 5 °C/min.

system over the studied temperature range. In other words, the binodals are all located below the gelation boundaries, which is evident from the binodal (curve "ABC") at 25 °C determined previously on the basis of the measured data for the PVDF terpolymer and the theoretical calculations.⁵ The binodals at higher temperatures are anticipated to be below curve "ABC". They depend, however, weakly on temperature; for example, measured liquid–liquid demixing points for PVDF terpolymer at 65 °C (i.e., open triangle points "S", "T", and "V") are only slightly lower than those measured at 25 °C (the dotted line). Such a weak temperature dependence phenomenon for the binodal has also been described by Soh¹⁶ and Young.¹³

The phase behavior of the water/DMF/PVDF system (Figure 1b) differs markedly from that of the 1-octanol/DMF/PVDF system; viz., the gelation curves intercept the binodals at elevated temperatures. At 25 and 45 °C, only crystallization-induced gelation was observed. As the temperature was increased to 65 °C, pure liquid–liquid demixing occurred in the low polymer concentration range, wherein the originally homogeneous solution is now separated into two clear liquid phases. In the high polymer concentration range, crystallization dominated and equilibrium gels were formed. As in the 1-octanol–DMF–PVDF system, the gelation boundaries at higher temperatures move downward in a manner roughly parallel to that at 25 °C. The binodal at 25 °C determined previously is shown as curve "ABC" in Figure 1b.¹⁴ It appears that the binodal is less sensitive to temperature changes than the gelation boundary as in the 1-octanol/DMF/PVDF system. As a result, these two phase boundaries begin to intersect each other at ca. 65 °C. Such a phenomenon has also been reported in other binary and ternary systems, e.g., the poly(vinyl alcohol)/ethylene glycol system by Stokes,¹⁷ the tallow-amine/iPP system by Lloyd,¹⁸ and the water/DMF/EVAL system by Young et al.¹³

Morphology of Membrane Prepared from 1-Octanol/DMF/PVDF System. The SEM photomicrographs of the membranes prepared by immersing casting dope "X" in 1-octanol bath at 25 and 65 °C are shown in Figures 3 and 4, respectively. The structure

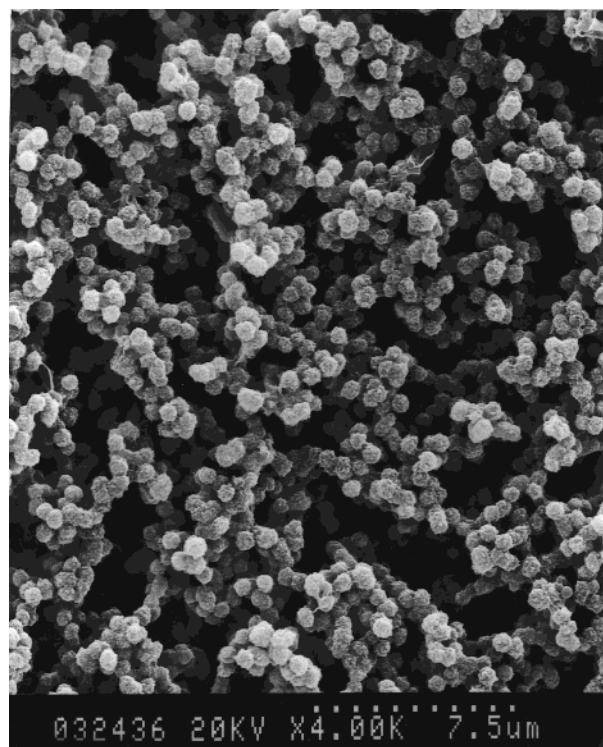


Figure 3. SEM photomicrographs of the membranes prepared by immersion of dope "X" in 1-octanol bath at 25 °C.

of the membrane prepared at 45 °C is similar to that at 25 °C and is thus not shown here. Dope "X" was located between the gelation boundaries at 25 and 65 °C; hence, it was in an "incipient precipitation" state with respect to crystallization at 25 °C, but it remained in a solution state, when the temperature was raised to 65 °C.^{4,5,13,14} Figures 3 and 4 illustrate clearly the strong effect of temperature on membrane morphology. The membrane formed at 25 °C is uniform in all dimensions, being composed of spherical PVDF crystallites of roughly identical size.⁵ There is no evidence of the cellular structure that characterizes the liquid–liquid demixing process during precipitation. By contrast, the membrane prepared at 65 °C is asymmetric with a dense layer formed on the top surface, and its cross section demonstrates a cellular structure mixed with spherical particles. The morphological differences between these two membranes can be understood by referring to the phase behaviors at respective temperatures. From Figure 1a, the gap between the gelation curve and the binodal at 25 °C is very wide. Therefore, as an incipient-precipitation casting dope (e.g., "X") that is highly populated with prenucleation aggregates is immersed in the nonsolvent bath, crystallization can occur rapidly without involving liquid–liquid demixing. This point is clearly illustrated in the calculated diffusion trajectories and concentration profiles. As shown in Figure 5, the binodal is crossed at 8 min after immersion. However, the membrane solution became a soft gel and could be removed from the glass plate at 1 min after immersion. In other words, the membrane solution is located outside the binodal, and its concentration is largely constant during the precipitation process. This explained why liquid–liquid demixing was totally suppressed and why crystallization dominated the precipitation process to yield the particulate structure shown in Figure 3. The particles are crystallites of PVDF, as is confirmed by the X-ray diffraction scans shown in curve "A" of Figure 6.

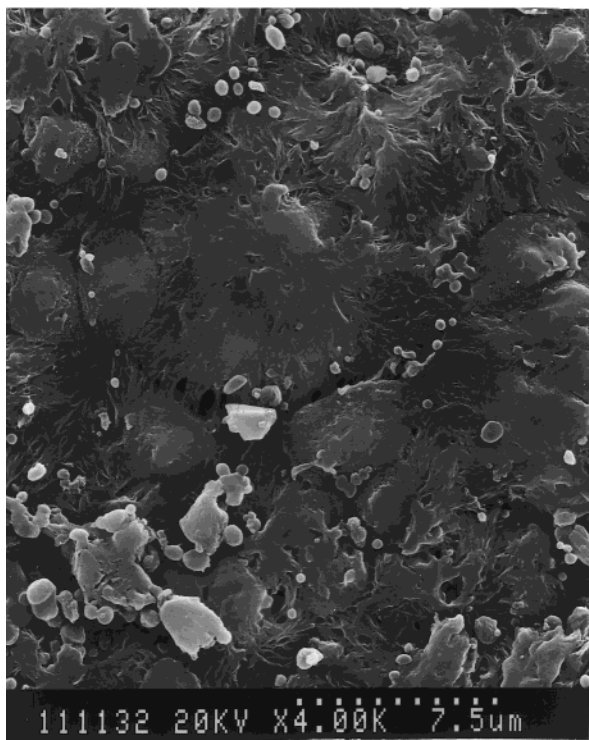
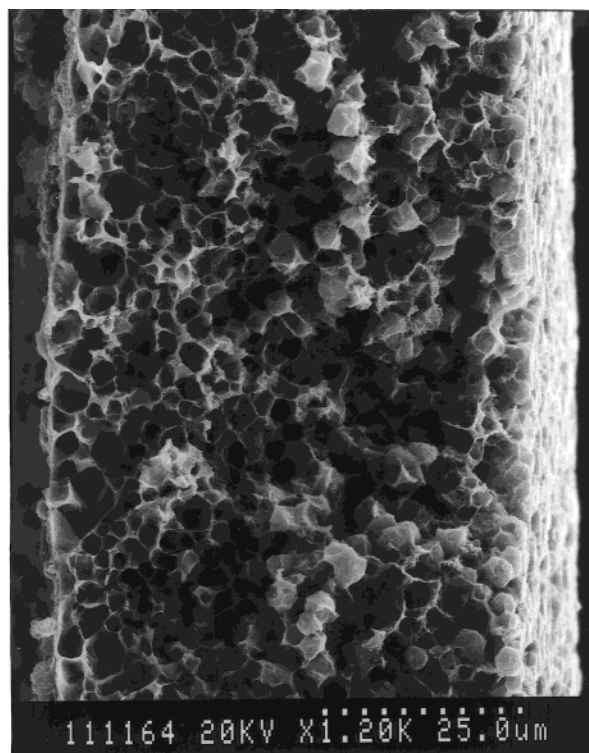


Figure 4. SEM photomicrographs of the membranes prepared by immersion of dope "X" in 1-octanol bath at 65 °C: (a, top) cross section; (b, bottom) top surface.

Compared with the crystallographic data of PVDF from the literature, it appears that the PVDF crystallites here are a mixture of " α " and " β " forms (largely in " β " form) that are arranged in an orthorhombic unit cell. The peak at 20.66° can be attributed to the reflection of the (110) plane.^{19,20}

At 65 °C, the gap between the phase boundaries became relatively small and dope "X" was in a good dissolution state. This provided a favorable condition

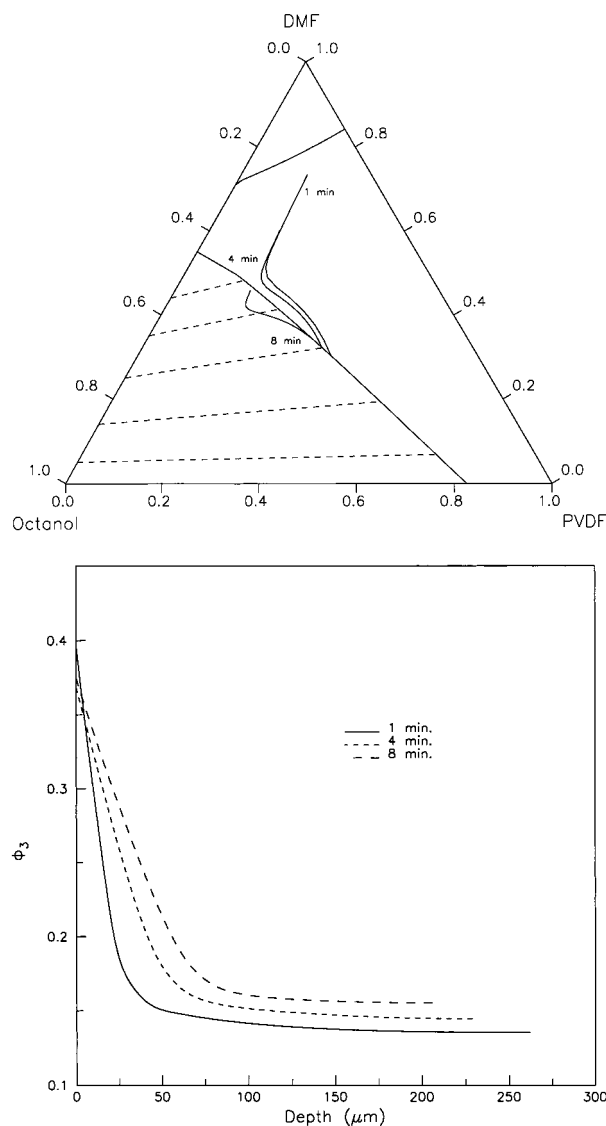


Figure 5. Computed diffusion trajectory and concentration profile for immersing dope "X" in 1-octanol at 25 °C. Compositions are in volume fractions.

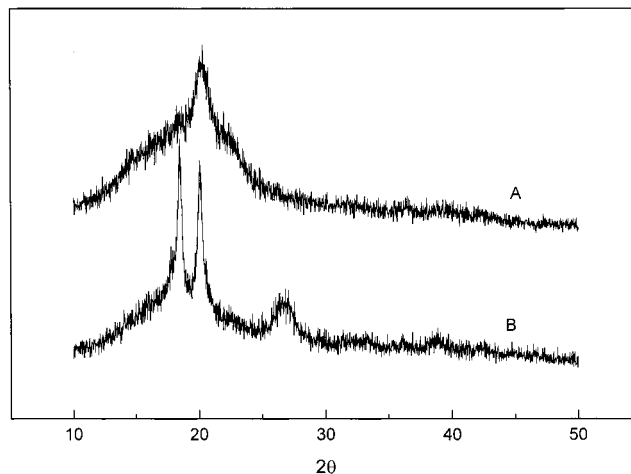


Figure 6. WAXD data of membranes prepared by immersion of dope "X" in 1-octanol at (a) 25 and (b) 65 °C. X-ray (Cu-K α) wavelength was 1.540 56 Å.

for the binodal to be entered and liquid–liquid demixing initiated before crystallization, which is evident from the SEM photomicrograph of the membrane cross

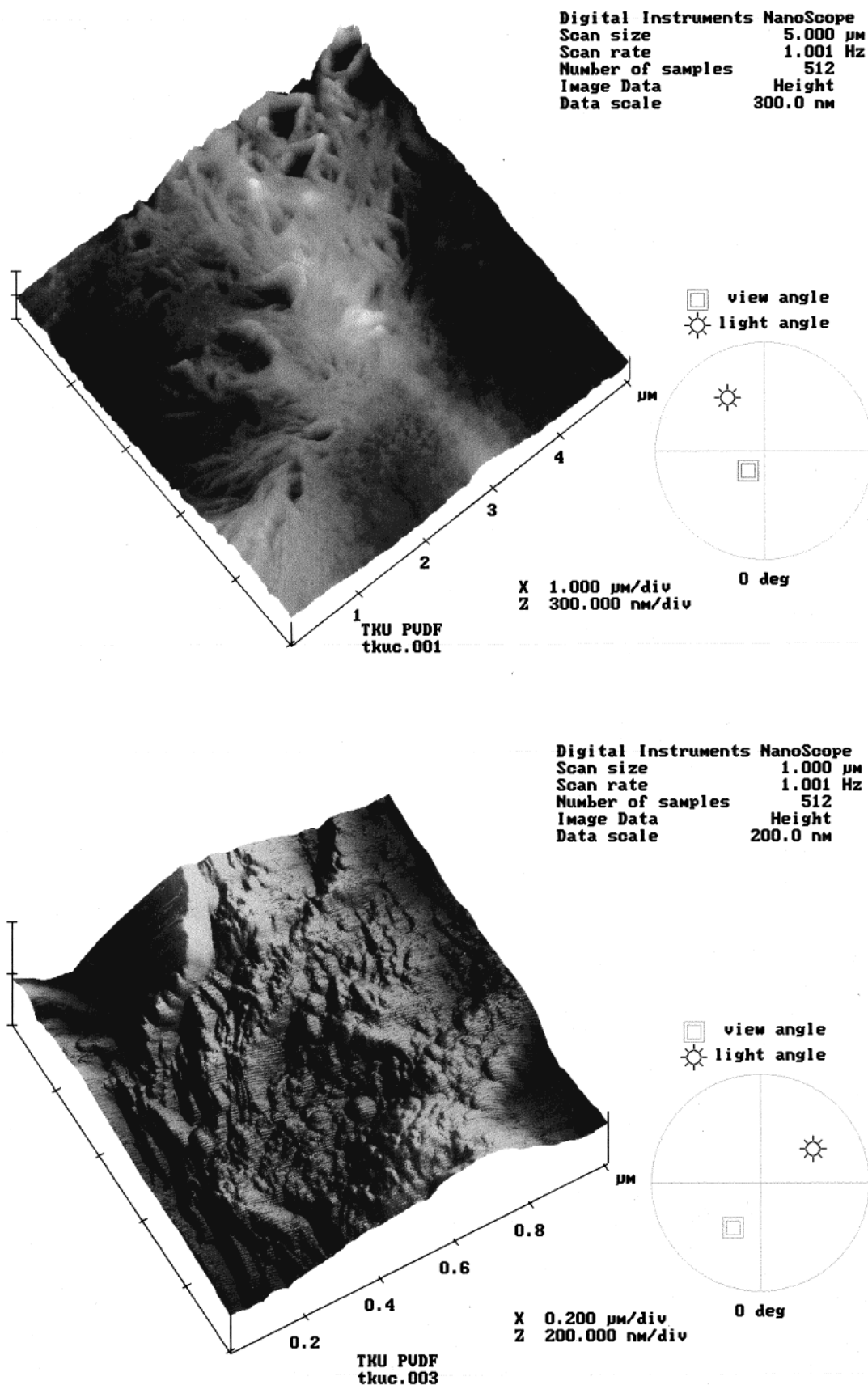


Figure 7. AFM images of the top surface of membrane shown in Figure 4.

section shown in Figure 4. The cellular morphology formed by growth of liquid micelles against the concentrated phase constituted most of the membrane cross section. There is some trace of particulate structure

toward the bottom region. Crystallization left much of its imprints on the top surface where liquid-liquid demixing was not possible. As is observed from Figure 4b, the top skin consists of polygonal crystalline units

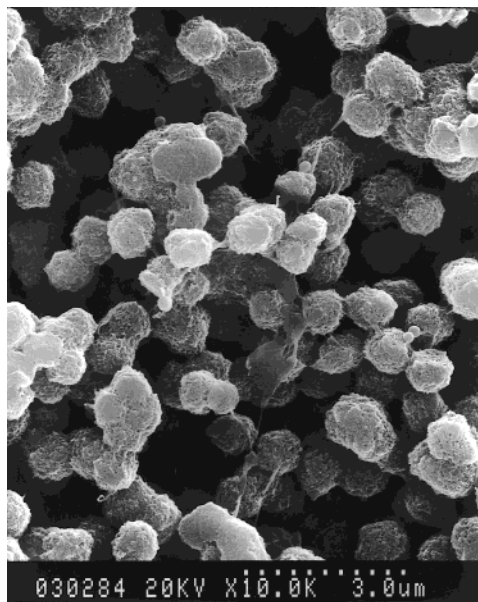


Figure 8. SEM photomicrographs of the membranes prepared by immersion of dope "W" in water bath at 25 °C.

that break into dendritic structure resembling two-dimensional spherulites. The lamellae of the crystallites can easily be identified by AFM imaging. In Figure 7, two different magnifications of the PVDF dendrites are presented. The lamellar structure can clearly be observed from the higher magnification image (Figure 7b). The interlamellar distance was determined to be ca. 13–20 nm (measured by the phase contrast mode for different regions), which is close to the results reported in the literature measured by TEM and SAXS techniques.^{21–23} The X-ray diffraction pattern of the membrane, as shown in diffraction line "B" in Figure 6, represents a typical " α " structure of the PVDF crystallite, which differs from the membrane formed at 25 °C (i.e., line "A" in Figure 6). The three characteristic peaks at 18.44°, 20.13°, and 26.73° are assigned to the reflections from (200), (110), and (201) planes, respectively.

Morphologies of Membranes Prepared from Water/DMF/PVDF System. For the water/DMF/PVDF system, temperature affects membrane formation following a trend similar to that for the 1-octanol/DMF/PVDF system; viz., high temperature favors liquid–liquid demixing. The morphologies of the membranes formed at 25 and 65 °C are presented in Figures 8 and 9, respectively. The casting dope (i.e., point "W" in Figure 1b) was a good solution at 65 °C, yet highly supersaturated at 25 °C, similar to the situation of dope "X" for the 1-octanol/DMF/PVDF system. The nonsolvent bath, containing 75 wt % DMF in water, was very weak with respect to polymer precipitation. The purpose of using this bath was to sufficiently suppress the liquid–liquid demixing process, which was made possible by slowing down the mass exchange of solvent and nonsolvent across the interface.¹⁴ Hence, before the membrane solution entered the binodal to initiate liquid–liquid demixing, crystallization started quickly in the "incipient dope" and dominated the precipitation process. This was the case even when the crystallization zone between gelation and binodal boundaries was relatively small at 25 °C (cf. Figure 1b). The formed membrane, as shown in Figure 8, exhibited a typical particulate morphology similar to that shown previously in Figure 3. If the nonsolvent bath is changed to water

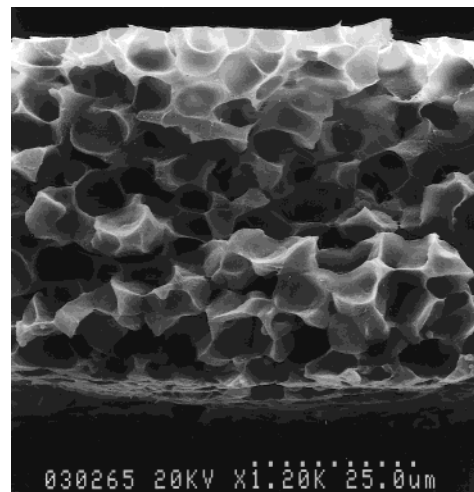


Figure 9. SEM photomicrographs of the membranes prepared by immersion of dope "W" in water bath at 65 °C.

(harsh bath for PVDF), the formed membrane will give an asymmetric structure like ordinary amorphous membranes.¹⁴

The membrane formed at 65 °C demonstrated a cellular morphology. As shown in Figure 9, it is composed of large cellular pores similar to those of common amorphous membranes. This indicates that liquid–liquid demixing has dominated the initiation stage of the precipitation process. The phase diagram at 65 °C in Figure 1b indicates that the binodal and gelation phase boundaries intersect each other, and there is a pure liquid–liquid demixing region above the gelation line. As a result, the casting membrane solution (point "W", a good solution) could enter the binodal easily to trigger liquid–liquid demixing, even though the bath was very soft and the mass transfer was thought to be slow. Only after liquid–liquid demixing, the gel layer that surrounds the cellular pores can crystallize to form the cell walls.

Conclusion

An attempt has been made to correlate the membrane morphology with the phase behavior of the membrane forming water/DMF/PVDF and 1-octanol/DMF/PVDF systems. Phase diagrams, i.e., crystallization-induced gelation line and binodal, of these systems were determined over the range 25–85 °C. As the temperature was raised, the gelation region contracts significantly more than the liquid–liquid demixing region. This provided a favored condition for liquid–liquid demixing to take place earlier than crystallization, and thus cellular asymmetric morphologies were produced at elevated temperatures. At low temperatures, the membrane formed into a uniform particulate structure dominated by the crystallization mechanism, consistent with the trajectory calculations and the X-ray diffraction analysis.

Acknowledgment. The authors acknowledge Mr. Hansen Chen of Scientek Corp., Taiwan, for the many hours of careful attention given to the preparation of AFM images. Also, the authors thank Mr. Hsi-Yuan Yang, Ching-Yen Lin, and Chih-Yuan Tang of Advanced Instrumentation Center, National Taiwan University, for SEM imaging. This research is supported by National Council of Taiwan ROC (NSC 87-2216-E-032-001).

References and Notes

- (1) Bulte, M. W.; Mulde, M. H. V.; Smolders, C. A.; Strathmann, H. *J. Membr. Sci.* **1996**, *121*, 37.
- (2) Bulte, M. W.; Mulde, M. H. V.; Smolders, C. A.; Strathmann, H. *J. Membr. Sci.* **1996**, *121*, 51.
- (3) Witte, P. V.; Esselbrugge, H.; Dijkstra, P. J.; Feijen, J.; Berg, W. A. *J. Polym. Sci.; Part B: Polym. Phys.* **1996**, *34*, 2553.
- (4) Cheng, L. P.; Dwan, A. W.; Gryte, C. C. *J. Polym. Sci., Polym. Phys.* **1995**, *33*, 211.
- (5) Cheng, L. P.; Young, T. H.; Fang, L.; Gau, J. J. *Polymer* **1999**, *40*, 2395.
- (6) Cheng, L. P.; Young, T. H.; You, Y. M. *J. Membr. Sci.* **1998**, *145*, 77.
- (7) Strathmann, H. In *Material Science of Synthetic Membrane*; Lloyd, D. R., Ed.; ACS Symposium Series; American Chemical Society: Washington, DC, 1985.
- (8) Smolders, C. A. *J. Membr. Sci.* **1992**, *73*, 259.
- (9) McKelvey, S. A.; Koros, W. J. *J. Membr. Sci.* **1996**, *112*, 29.
- (10) Kesting, R. E. *Synthetic Polymeric Membranes*; John Wiley & Sons: New York, 1985.
- (11) Tsay, C. S.; McHugh, A. J. *J. Polym. Sci., Polym. Phys.* **1990**, *28*, 1327.
- (12) Bottino, A.; Roda Camera, G.; Capannelli, G.; Munari, S. *J. Membr. Sci.* **1991**, *57*, 1.
- (13) Young, T. H.; Cheng, L. P.; You, W. M.; Chen, L. Y. *Polymer* **1999**, *40*, 2189.
- (14) Cheng, L. P.; Lin, D. J.; Shih, C. H.; Dwan, A. W.; Gryte, C. C. PVDF membrane formation by diffusion induced phase separation—morphology prediction based on phase behavior and mass transfer modeling. *J. Polym. Sci.*, in press.
- (15) Young, T. H.; Cheng, L. P.; Lin, D. J.; Fane, L.; Chuang, W. Y. *Polymer*, in press.
- (16) Soh, Y. S.; Kim, J. H.; Gryte, C. C. *Polymer* **1995**, *36*, 3711.
- (17) Stokes, W.; Berghmans, H. *J. Polym. Sci., Polym. Phys.* **1991**, *29*, 609.
- (18) Lloyd, D. R.; Kim, S. S.; Kinzer, K. E. *J. Membr. Sci.* **1991**, *64*, 1.
- (19) Lovinger, A. J. In *Developments in Crystalline Polymers-1*; Bassett, D. C., Ed.; Applied Science Publisher: Oxford, 1988; Chapter 5.
- (20) Davis, G. T.; McKinney, J. E.; Broadhurst, M. G.; Roth, S. C. *J. Appl. Phys.* **1978**, *49*, 4998.
- (21) Nakagawa, K.; Ishida, Y. *J. Polym. Sci., Polym. Phys.* **1973**, *11*, 2153.
- (22) Wunderlich, B. *Macromolecular Physics*; Academic Press: New York, 1973; Vol. 1.
- (23) Cakmak, M.; Teitge, A.; Zachmann, H. G.; White, J. L. *J. Polym. Sci., Polym. Phys.* **1993**, *31*, 371.

MA990418L